UNCREWED AERIAL VEHICLES: AN INVESTIGATION OF THE PARAMETER INFLUENCES FOR COASTAL MONITORING

Marco Luppichini, Marco Paterni, Monica Bini

Abstract: Data and information obtained from low-cost uncrewed aerial vehicles (UAVs), commonly called 'drones', can be used to support coastal monitoring on erosion study. The Structure from Motion (SfM) techniques allow to reconstruction of a high-resolution Digital Elevation Model (DEM) useful to assess shoreline e dune mass, starting from the images acquired by UAVs. Flight procedures, acquisition methods and ground references are important parameters to be carefully managed to achieve the necessary accuracy. However, the size of the areas to be monitored and the frequency of measurements require demanding resources that can limit studies when they are insufficient. This work aims to investigate the best flight and processing settings for applying SfM for coastal monitoring. The parameters investigated are for example the drone type, flight height, ground control points (GCPs) position and post-processing parameters. The results of these evaluations and the proposed procedure are shown

Keywords: Coastal Monitoring, Drones, Structure from Motion

Marco Luppichini, University of Pisa, Italy, marco.luppichini@dst.unipi.it, 0000-0002-0913-3825
Marco Paterni, Clinical Physiology Institute CNR, Italy, marco.paterni@ifc.cnr.it, 0000-0002-9799-7059
Monica Bini, University of Pisa, Italy, monica.bini@unipi.it, 0000-0003-1482-2630

Referee List (DOI 10.36253/fup_referee_list)
FUP Best Practice in Scholarly Publishing (DOI 10.36253/fup_best_practice)

Marco Luppichini, Marco Paterni, Monica Bini, *Uncrewed aerial vehicles: an investigation of the parameter influences for coastal monitoring*, pp. 761-772, © 2024 Author(s), CC BY-NC-SA 4.0, DOI: 10.36253/979-12-215-0556-6.66

Introduction

In recent years, the use of Unmanned Aerial Vehicles (UAVs) for high-resolution topographic surveys has increased significantly, yielding excellent results across various environments [1–9]. Among the techniques employed for topographic reconstruction using drones, photogrammetric surveys are the most used [10–21]. However, several factors can impact the accurate reconstruction of geometries within a model, including flat areas, water presence, and the availability of unidirectional models.

Coastal environments, in particular, exhibit all three of these factors, making them challenging terrain for Structure from Motion (SfM) models. SfM models play a crucial role in coastal monitoring, allowing quantification of seasonal variations, storm surge impacts, and human activities [5,6,8,22–27].

One way to enhance SfM models is through the use of ground control points (GCPs) for georeferencing and geometry reconstruction [17,28,29]. GCPs also help estimate errors in the three dimensions of the model, which is essential for understanding uncertainty in subsequent processing phases. However, the optimal number of GCPs required for precise and repeatable results over time remains scientifically unclear.

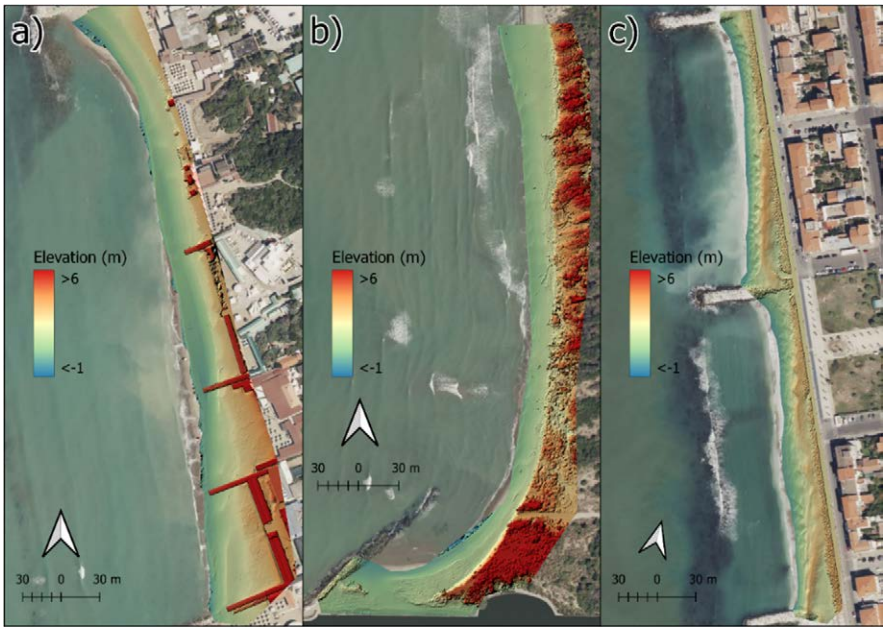

Figure 1 – Topographic characteristics of the three areas. The images contain Digital Elevation Models (DEMs) derived by DJI Phantom 4 at 30 m and using 20 GCPs for georeferencing: a) Area 1; b) Area 2, c) Area 3. Base map provided by Bing.

In this study, we analyze the effects of GCP positioning in three distinct coastal environments: low sandy beach (Area 1), sandy beach with dunes and vegetation (Area 2), and pebble beach with anthropic structures (Area 3: Figure 1). By sampling these areas using two drones at different flight heights and varying the number of GCPs during post-processing, we investigate error variations both spatially and in terms of average values.

Materials and Methods

The three study areas were surveyed using a DJI Phantom 4 Pro V2 and a DJI Mini 2. Flight plans for the DJI Phantom 4 were created using PIX4D Capture software, while for the DJI Mini 2, the Map Creator app for iOS was used. The flight plans were designed to achieve an 80 % overlap between acquired photos on each side and a pitch of 90° (orthogonal to the ground). Sampling campaigns were conducted at three flight heights: 30 m, 50 m, and 70 m.

The use of the DJI Phantom 4 and DJI Mini 2 can lead to differences in photogrammetric results, primarily due to variations in camera quality, sensor size, and stabilization. Equipped with a higher-resolution sensor and a 3-axis gimbal, the DJI Phantom 4 enables more detailed and stable image capture, enhancing the quality of the final model. Additionally, its superior focal length and stabilization reduce distortion and blurring, positively impacting overall survey accuracy.

In each study area, we strategically positioned a substantial number of markers. Specifically, we placed 55 markers in Area 1, 41 markers in Area 2, and 46 markers in Area 3. The marker positions were sampled using a Differential GPS Emlid Reach 2 with Real-time Kinetic (RTK) positioning.

We applied the Structure from Motion (SfM) technique using Metashape Professional v. 2.0.4. The analysis focused on error metrics provided by Agisoft Metashape for both control and checkpoint markers. The evaluation of the accuracy of the models is provided by calculating the Root Mean Square Errors (RMSE), as follows:

$$RMSE = \sqrt{\frac{1}{N}\sum_{i=1}^{N}((X_i - \overline{X}_\iota)^2 + (Y_i - \overline{Y}_\iota)^2 + (Z_i - \overline{Z}_\iota)^2)}$$

where N is the number of control points; X_i, Y_i, Z_i are the observed coordinates of the i-th point; $\overline{X}_\iota,\ \overline{Y}_\iota, \overline{Z}_\iota$ are the coordinates calculated by the model for the i-th point.

We systematically varied the number of control points, starting from three points (a minimum number to georeference a three-dimensional model) and gradually incorporating the full set of markers positioned in each study area. The marker not used as control points are used as check points. The first step use three markers as control points, the second step use four markers as control points and the procedure progress until the entire number of markers is used as control points. The choice of the markers used as control point is random. For this reason, the entire procedure is repeated thirty-five times generating more casual situations for a statistical analysis.

Results

The RMSE calculated for control points and check points related to changes in the Ground Control Points (GCPs) used are reported in Figure 3. As expected, the RMSE for control points is lower than that calculated for check points. The RMSE for control points shows a significant reduction when using 3 additional GCPs per hectare (equivalent to approximately 10 GCPs in the study areas).

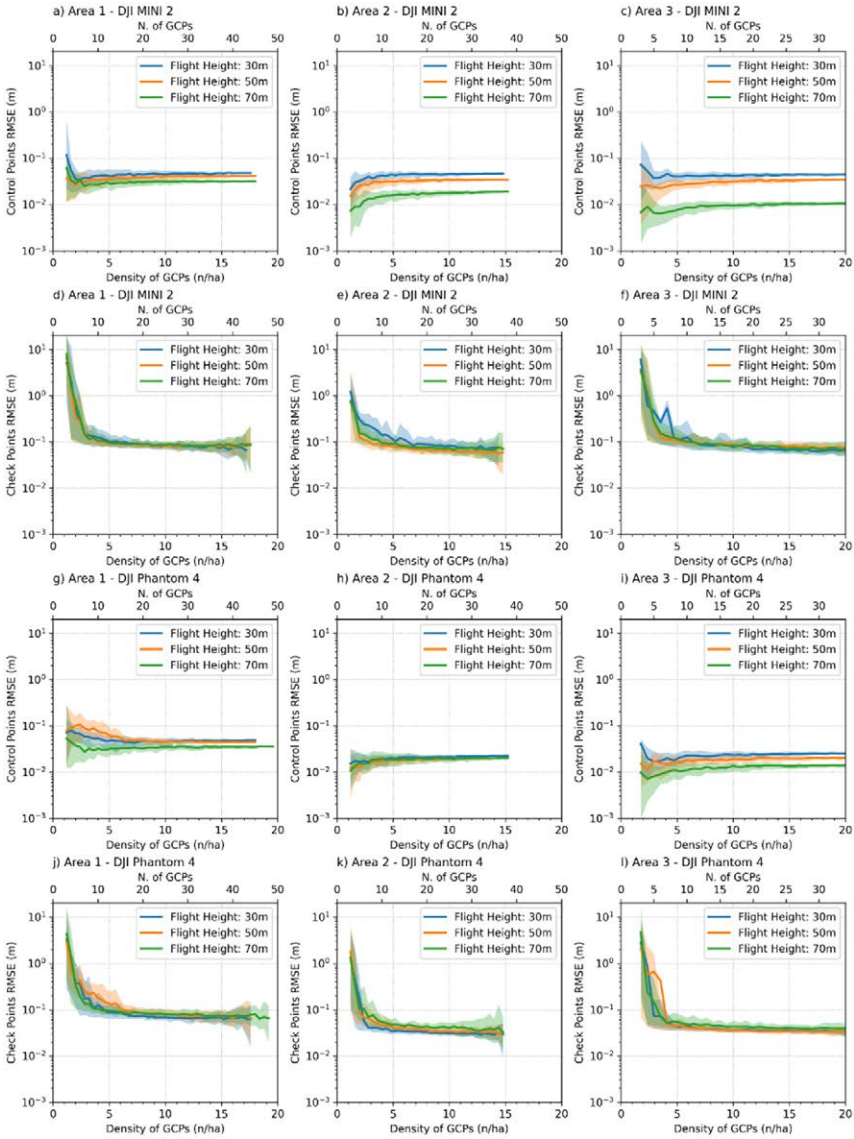

Figure 2 – Mean Square Errors (RMSE) of the control and check points.

In contrast, check points exhibit greater variability and require about 5 GCPs per hectare to achieve smaller errors. For Areas 2 and 3, the DJI Phantom 4 outperforms the DJI Mini 2, with the lowest RMSE observed for all flight heights. In Area 1, the two drones yield more comparable results, making it difficult to determine which equipment is superior. When using the DJI Mini 2, point clouds have the lowest RMSE for check points, approximately 7-10 cm across all investigated areas. The DJI Phantom 4 allows for point clouds with even lower RMSE (around 3-4 cm) for check points in Areas 2 and 3 (Figure 3).

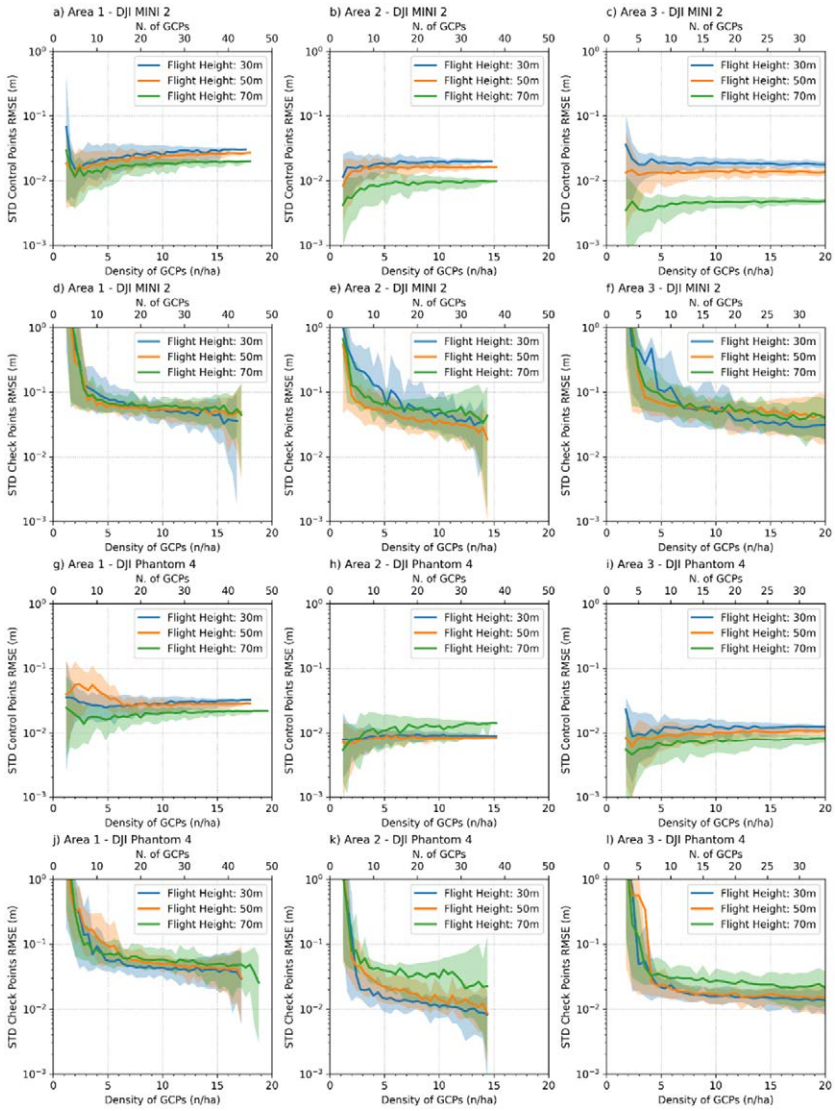

Figure 3 – Standard Deviation (STD) of the Square Errors of the control and check points.

The statistical mean of errors is an important parameter for assessing the quality of a photogrammetric model. However, it is equally crucial to investigate error variability along the model. This variability is influenced by factors such as control point positions, site topography, and the number of projections per marker (Figure 4). Even in this case, using more than 5 GCPs per hectare results in models with the lowest RMSE standard deviation for both control and check points, indicating less error variability. The DJI Phantom 4 achieves the lowest standard deviation values in Areas 2 and 3. Conversely, using the DJI Mini 2 introduces greater RMSE variability for both control and check points.

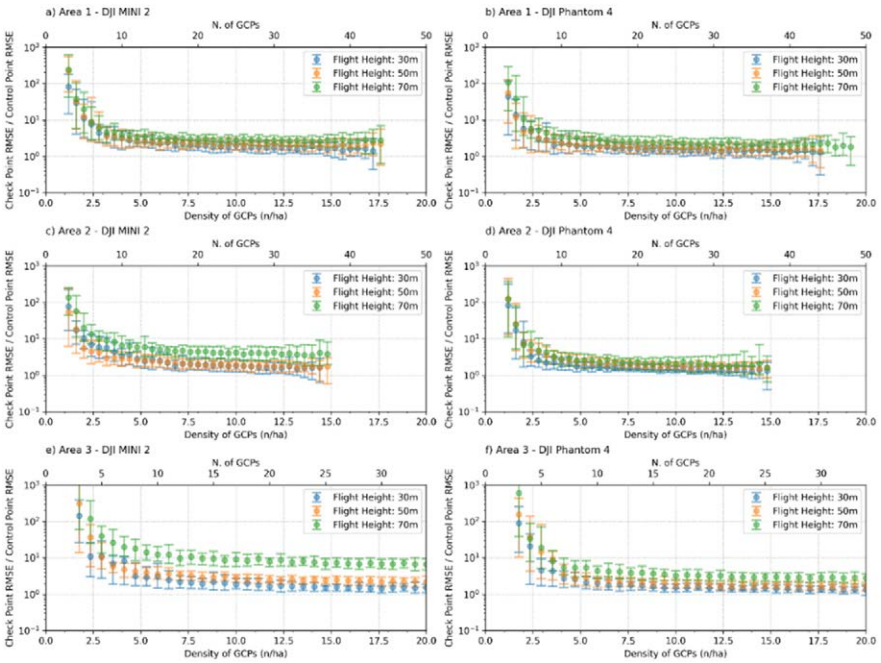

Figure 4 – Ratio between the RMSE checkpoint and the RMSE control point.

Ground Control Points (GCPs) were initially distributed evenly across the entire area of interest. For all the evaluated combinations, the selection of GCPs was random. However, since every combination was saved, it was possible to analyse the accuracy of the location of the GCPs. Figures 9 and 10 depict accuracy versus the average distance between GCPs (Figure 5) and the standard deviation of distances between GCPs (Figure 6). Averaged distances and standard deviations were calculated using all the GCPs employed in each combination.

Optimal accuracies for checkpoints were observed when GCPs within a specific combination had average distances of approximately 170 meters with standard deviations of about 100 meters. Remarkably, these values closely aligned with those obtained when statistics were calculated using all the GCPs. Averaged

distances below 170 meters were associated with situations where the GCPs did not cover peripheral areas. In contrast, averaged distances exceeding 170 meters indicated fewer points but a well-distributed coverage across the entire area. Regarding standard deviations, values below 100 meters indicated that points were preferably grouped in small areas, whereas higher values suggested larger gaps between GCPs. While it is unsurprising that maximum accuracy is achieved when every ground point serves as a control, we observed that RMSE values degraded when points were limited in number, poorly distributed, or widely separated.

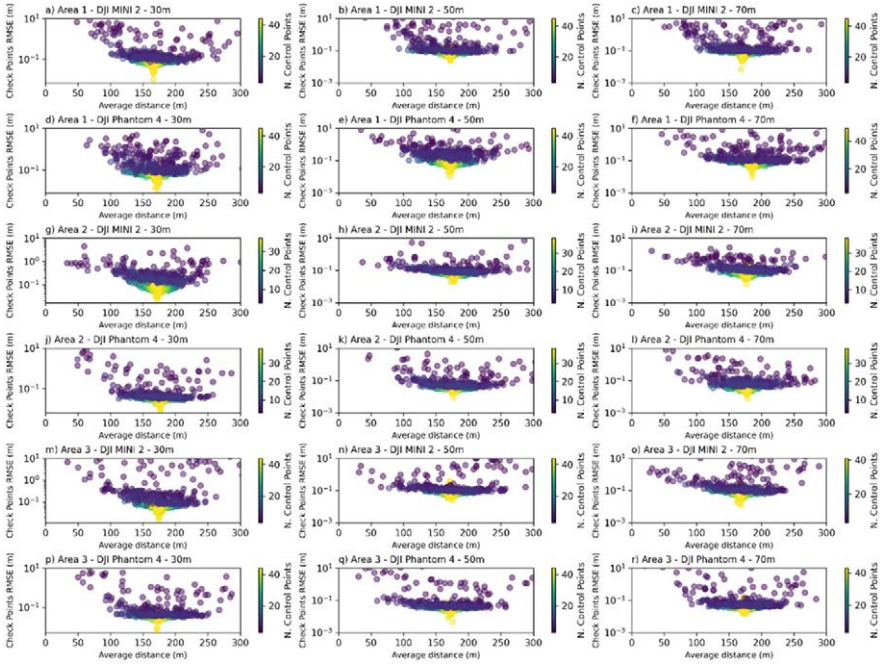

Figure 5 – Average distance between Control Point and Checkpoint Root Mean Square Errors (RMSE).

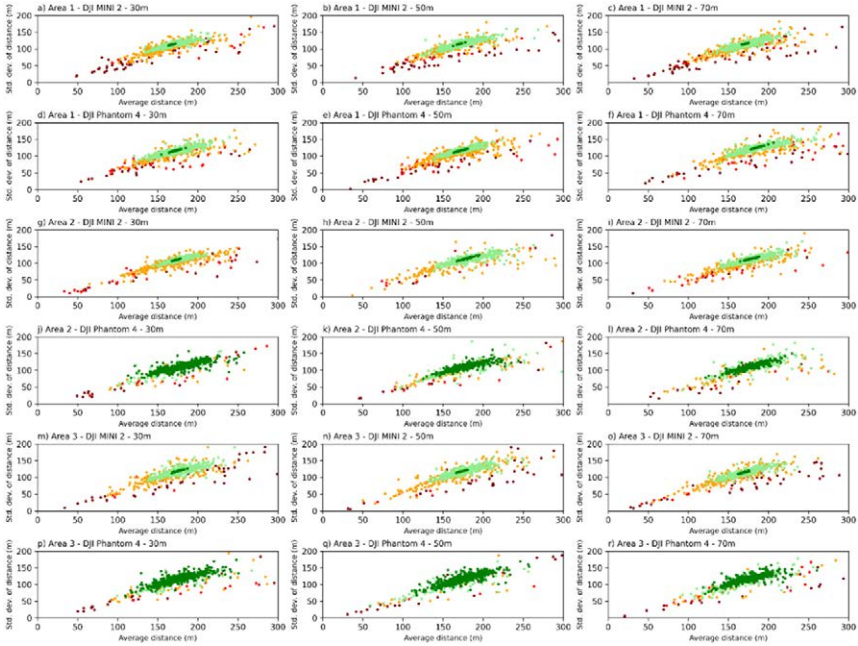

Figure 6 – Standard deviation of the distances between check points and Average distance between Control Points. The point colour indicates the Checkpoint Root Mean Square Errors (RMSE): the green points indicate an RMSE between 0 and 0.05 m; the light green points indicate an RMSE between 0.05 and 0.1m; the yellow points indicate an RMSE between 0.1 m and 0.5 m; the orange points indicate an RMSE between 0.5 m and 1 m; and the red points indicate an RMSE higher than 1 m.

Discussion and Conclusions

The geometric accuracy of the 3D SfM model strongly depends on the georeferencing strategy. The results of this study confirm that accuracy is influenced by the number of Ground Control Points (GCPs) used to adjust the point cloud. When using a small number of GCPs (fewer than 5 markers per hectare), the Root Mean Square Error (RMSE) at the checkpoint is very high, even exceeding several decimetres. Additionally, the variability along the model is also significant. However, by increasing the number of GCPs, the RMSE at the checkpoint decreases, reaching values lower than 10 cm, and the variability along the models decreases as well. This influence of GCPs on the models aligns with results from previous studies in other environments [17,30]. Both drones exhibit similar trends, but in two cases, the DJI Phantom 4 outperforms the DJI Mini 2, achieving a lower checkpoint error. These findings are consistent with results obtained in prior research [15,17,20,31,32].

It appears that further improvement of this value is not possible, regardless of the number of Ground Control Points (GCPs) used. Interestingly, flights at lower altitudes, which offer higher spatial resolution, exhibit accuracy comparable to that of flights at higher altitudes. One plausible reason for this phenomenon is that more distant points appear in a greater number of images, resulting in increased

redundancy [17]. This observation could also explain the varying results obtained across the three study areas. In Areas 2 and 3, the DJI Phantom 4 outperformed the DJI Mini 2, while the results were similar in Area 1. Notably, in Area 1, the flights conducted with the DJI Mini 2 had a higher number of projections for each marker compared to those conducted with the DJI Phantom 4. Additionally, the increased redundancy in the photos may suggest improved performance of the Structure-from-Motion (SfM) technique [33].

This study has demonstrated that optimal accuracies are achieved when GCPs are uniformly distributed across the entire area. Strategies such as concentrating GCPs in specific areas, leaving gaps without GCPs, or focusing points on the periphery or centre do not yield good accuracy [17, 30, 34]. Ideally, the distribution of GCPs should follow a triangular grid, minimizing the maximum distance of each point to the nearest GCP.

When evaluating the geometric accuracy of a 3D model obtained through Structure-from-Motion (SfM), relying solely on ground points used as control is insufficient. This becomes critical when the number of GCPs is limited. While the RMSE (Root Mean Square Error) calculated at control points may appear extremely low (sometimes only a few millimetres) when using only a few points for control, a deeper analysis reveals that the actual RMSEs of the checkpoints can be much higher, even exceeding several decimetres. With a limited number of GCPs, the 3D model can adapt to the few geometric constraints introduced, resulting in low control residuals. However, increasing the number of GCPs reduces the ratio between RMSE at control points and RMSE at checkpoints, stabilizing at around 5 GCPs per hectare (Figure 4).

Figure 4 provides insights into estimating the RMSE at checkpoints when the number of markers is insufficient for control and checkpoint usage. Additionally, analyzing the Standard Deviation of the RMSE can enhance the assessment. Despite low variability in RMSE at control points with a small number of GCPs (as seen in Figure 3), the RMSE at checkpoints can still be significantly higher.

In summary, when using a small number of Ground Control Points (GCPs), the 3D models can be affected by high and variable RMSE (Root Mean Square Error) at checkpoints, while the RMSE at control points remains lower and less variable. This discrepancy can lead to an incorrect interpretation of result quality.

The study findings suggest that more than 5 markers per hectare (markers/ha) are necessary to achieve consistent and low errors. Interestingly, this requirement holds across different site characteristics (as observed in three distinct study areas) and regardless of the performance of the two different drones used.

In coastal environments, Structure-from-Motion (SfM) exhibits variability in error distribution along the model. Therefore, whenever feasible, it is crucial to associate a Digital Elevation Model (DEM) with an error map. This consideration becomes especially important during topographic and morphological analyses.

For future research, investigating the effects of other parameters—such as camera pre-calibration, which can reduce systematic errors in image alignment, and pitch angle adjustments, which may improve image overlap and coverage in complex coastal topography—could significantly enhance the accuracy and reliability of SfM models. These factors are especially important in coastal environments, where accurate topographic data is essential for understanding geomorphological changes.

References

[1] Dietrich, J. (2014) - *Applications of Structure-from-Motion Photogrammetry to Fluvial Geomorphology*. PhD, University of Oregon: Oregon,.

[2] Dietrich, J.T. (2017) - *Bathymetric Structure-from-Motion: Extracting Shallow Stream Bathymetry from Multi-View Stereo Photogrammetry*. Earth Surf Process Landf, 42, 355–364, DOI:10.1002/esp.4060.

[3] Dietrich, J.T. (2016) - *Riverscape Mapping with Helicopter-Based Structure-from-Motion Photogrammetry*. Geomorphology, 252, 144–157, DOI: 10.1016/j.geomorph.2015.05.008.

[4] Carrera-Hernández, J.J.; Levresse, G.; Lacan, P. (2020) - *Is UAV-SfM Surveying Ready to Replace Traditional Surveying Techniques?* Int J Remote Sens, 41, 4820–4837, DOI: 10.1080/01431161.2020.1727049.

[5] Chen, B.; Yang, Y.; Wen, H.; Ruan, H.; Zhou, Z.; Luo, K.; Zhong, F. (2018) - *High-Resolution Monitoring of Beach Topography and Its Change Using Unmanned Aerial Vehicle Imagery*. Ocean Coast Manag, 160, 103–116, DOI: 10.1016/j.ocecoaman.2018.04.007.

[6] Gonçalves, J.A.; Henriques, R. (2015) - *UAV Photogrammetry for Topographic Monitoring of Coastal Areas.* ISPRS Journal of Photogrammetry and Remote Sensing, 104, 101–111, DOI: 10.1016/j.isprsjprs.2015.02.009.

[7] Clapuyt, F.; Vanacker, V.; Van Oost, K. (2016) - *Reproducibility of UAV-Based Earth Topography Reconstructions Based on Structure-from-Motion Algorithms*. Geomorphology, 260, 4–15, DOI: 10.1016/j.geomorph.2015.05.011.

[8] Turner, I.L.; Harley, M.D.; Drummond, C.D. (2016) - *UAVs for Coastal Surveying*. Coastal Engineering, 114, 19–24, DOI: 10.1016/j.coastaleng.2016.03.011.

[9] Westoby, M.J.; Brasington, J.; Glasser, N.F.; Hambrey, M.J.; Reynolds, J.M. (2012) - *'Structure-from-Motion' Photogrammetry: A Low-Cost, Effective Tool for Geoscience Applications.* Geomorphology, 179, 300–314, DOI: 10.1016/j.geomorph.2012.08.021.

[10] Bertin, S.; Stéphan, P.; Ammann, J. (2022) - *Assessment of RTK Quadcopter and Structure-from-Motion Photogrammetry for Fine-Scale Monitoring of Coastal Topographic Complexity*. Remote Sens (Basel), 14, DOI:10.3390/rs14071679.

[11] Jugie, M.; Gob, F.; Virmoux, C.; Brunstein, D.; Tamisier, V.; Le Coeur, C.; Grancher, D. (2018) - C*haracterizing and Quantifying the Discontinuous Bank Erosion of a Small Low Energy River Using Structure-from-Motion Photogrammetry and Erosion Pins*. J Hydrol (Amst), 563, 418–434, DOI: 10.1016/j.jhydrol.2018.06.019.

[12] Kaiser, A.; Neugirg, F.; Rock, G.; Müller, C.; Haas, F.; Ries, J.; Schmidt, J. (2014) -*Small-Scale Surface Reconstruction and Volume Calculation of Soil Erosion in Complex Moroccan Gully Morphology Using Structure from Motion*. Remote Sens (Basel), 6, 7050–7080, DOI:10.3390/rs6087050.

[13] Luppichini, M.; Favalli, M.; Isola, I.; Nannipieri, L.; Giannecchini, R.; Bini, M. (2019) -*Influence of Topographic Resolution and Accuracy on Hydraulic Channel Flow Simulations: Case Study of the Versilia River (Italy)*. Remote Sens (Basel), 11, DOI:10.3390/rs11131630.

[14] Luppichini, M.; Bini, M.; Paterni, M.; Berton, A.; Merlino, S. (2020) - *A New Beach Topography-Based Method for Shoreline Identification. Water (Switzerland)*, 12, 1–11, DOI:10.3390/w12113110.

[15] Mancini, F.; Dubbini, M.; Gattelli, M.; Stecchi, F.; Fabbri, S.; Gabbianelli, G. (2013) - *Using Unmanned Aerial Vehicles (UAV) for High-Resolution Reconstruction of Topography: The Structure from Motion Approach on Coastal Environments*. Remote Sens (Basel), 5, 6880–6898, DOI:10.3390/rs5126880.

[16] Meesuk, V.; Vojinovic, Z.; Mynett, A.E.; Abdullah, A.F. (2015) - *Urban Flood Modelling Combining Top-View LiDAR Data with Ground-View SfM Observations*.

Adv Water Resour, 75, 105–117, DOI: 10.1016/j.advwatres.2014.11.008.

[17] Sanz-Ablanedo, E.; Chandler, J.H.; Rodríguez-Pérez, J.R.; Ordóñez, C. (2018) - *Accuracy of Unmanned Aerial Vehicle (UAV) and SfM Photogrammetry Survey as a Function of the Number and Location of Ground Control Points Used*. Remote Sens (Basel), 10, DOI:10.3390/rs10101606.

[18] Sedrati, M.; Morales, J.A.; El M'rini, A.; Anthony, E.J.; Bulot, G.; Le Gall, R.; Tadibaght, A. (2022) - *Using UAV and Structure-From-Motion Photogrammetry for the Detection of Boulder Movement by Storms on a Rocky Shore Platform in Laghdira, Northwest Morocco*. Remote Sens (Basel), 14, DOI:10.3390/rs14164102.

[19] Sturdivant, E.J.; Lentz, E.E.; Thieler, E.R.; Farris, A.S.; Weber, K.M.; Remsen, D.P.; Miner, S.; Henderson, R.E. (2017) - *UAS-SfM for Coastal Research: Geomorphic Feature Extraction and Land Cover Classification from High-Resolution Elevation and Optical Imagery*. Remote Sens (Basel), 9, DOI:10.3390/rs9101020.

[20] Taddia, Y.; Corbau, C.; Zambello, E.; Pellegrinelli, A. (2019) - U*AVs for Structure-From-Motion Coastal Monitoring: A Case Study to Assess the Evolution of Embryo Dunes over a Two-Year Time Frame in the Po River Delta, Italy*. Sensors, 19, DOI:10.3390/s19071717.

[21] James, M.R.; Robson, S.; d'Oleire-Oltmanns, S.; Niethammer, U. (2017) - *Optimising UAV Topographic Surveys Processed with Structure-from-Motion: Ground Control Quality, Quantity and Bundle Adjustment*. Geomorphology, 280, 51–66, DOI: 10.1016/j.geomorph.2016.11.021.

[22] Grottoli, E.; Biausque, M.; Rogers, D.; Jackson, D.W.T.; Cooper, J.A.G. (2021) - *Structure-from-Motion-Derived Digital Surface Models from Historical Aerial Photographs: A New 3D Application for Coastal Dune Monitoring*. Remote Sens (Basel), 13, DOI:10.3390/rs13010095.

[23] Scarelli, F.M.; Sistilli, F.; Fabbri, S.; Cantelli, L.; Barboza, E.G.; Gabbianelli, G. (2017) - *Seasonal Dune and Beach Monitoring Using Photogrammetry from UAV Surveys to Apply in the ICZM on the Ravenna Coast (Emilia-Romagna, Italy*). Remote Sens Appl, 7, 27–39, DOI: 10.1016/j.rsase.2017.06.003.

[24] Talavera, L.; Del Río, L.; Benavente, J.; Barbero, L.; López-Ramírez, J.A. (2018) - U*AS as Tools for Rapid Detection of Storm-Induced Morphodynamic Changes at Camposoto Beach, SW Spain*. Int J Remote Sens, 39, 5550–5567, DOI:10.1080/01431161.2018.1471549.

[25] Knight, J.; Burningham, H.; Griffiths, D.; Yao, Y. (2023) - *Coastal Boulder Movement on a Rocky Shoreline in Northwest Ireland from Repeat UAV Surveys Using Structure from Motion Photogrammetry*. Geomorphology, 440, 108883, DOI: 10.1016/j.geomorph.2023.108883.

[26] Omidiji, J.; Stephenson, W.; Norton, K. (2023) - *Cross-Scale Erosion on Shore Platforms Using the Micro-Erosion Meter and Structure-from-Motion (SfM) Photogrammetry*. Geomorphology, 434, 108736, DOI: 10.1016/j.geomorph.2023.108736.

[27] Terwisscha van Scheltinga, R.C.; Coco, G.; Kleinhans, M.G.; Friedrich, H. (2020) - *Observations of Dune Interactions from DEMs Using Through-Water Structure from Motion*. Geomorphology, 359, 107126, DOI: 10.1016/j.geomorph.2020.107126.

[28] Tonkin, T.N.; Midgley, N.G. (2016) - *Ground-Control Networks for Image Based Surface Reconstruction: An Investigation of Optimum Survey Designs Using UAV Derived Imagery and Structure-from-Motion Photogrammetry*. Remote Sens (Basel), 8, DOI:10.3390/rs8090786.

[29] Zhang, H.; Aldana-Jague, E.; Clapuyt, F.; Wilken, F.; Vanacker, V.; Van Oost, K. (2019) - *Evaluating the Potential of Post-Processing Kinematic (PPK) georeferencing for UAV-Based Structure-from-Motion (SfM) Photogrammetry and Surface Change*. Earth Surface Dynamics, 7, 807–827, DOI:10.5194/esurf-7-807-2019.

[30] Martínez-Carricondo, P.; Agüera-Vega, F.; Carvajal-Ramírez, F.; Mesas-Carrascosa, F.-J.; García-Ferrer, A.; Pérez-Porras, F.-J. (2018) - *Assessment of UAV-Photogrammetric Mapping Accuracy Based on Variation of Ground Control Points.* International Journal of Applied Earth Observation and Geoinformation, 72, 1–10, DOI: 10.1016/j.jag.2018.05.015.

[31] Harwin, S.; Lucieer, A. (2012) - *Assessing the Accuracy of Georeferenced Point Clouds Produced via Multi-View Stereopsis from Unmanned Aerial Vehicle (UAV) Imagery*. Remote Sens (Basel), 4, 1573–1599, DOI:10.3390/rs4061573.

[32] Novais, J.; Vieira, A.; Bento-Gonçalves, A.; Silva, S.; Folharini, S.; Marques, T. (2023) - *The Use of UAVs for Morphological Coastal Change Monitoring—A Bibliometric Analysis*. Drones, 7, DOI:10.3390/drones7100629.

[33] Guidi, G.; Micoli, L.L.; Gonizzi, S.; Brennan, M.; Frischer, B. (2015) - *Image-Based 3D Capture of Cultural Heritage Artifacts an Experimental Study about 3D Data Quality*. In Proceedings of the 2015 Digital Heritage; Vol. 2, pp. 321–324.